Applications of Multiscale and Subcycling methods for Press Hardened Steel parts failure assessment

Y. Drouadaine[1], P. Dietsch[2], S. Gaied[1], D. Hasenpouth[1]

[1]ArcelorMittal, Global R&D Montataire, France
[2]ArcelorMittal, Global R&D Maizières-lès-Metz, France

1 Introduction

In order to achieve both safety and environmental regulation objectives, car makers are largely using hot stamping technologies. Indeed, thanks to its unique combination of very good hot-forming and very high tensile strength properties, Usibor®1500 is a key material from ArcelorMittal steel offer to reduce Body in White (BIW) mass.
The increase of tensile strength is generally associated with a loss of ductility compared to more conventional steel grades, and the prediction of their failure in crash loading conditions becomes of great importance for the design of current vehicles.
Therefore, in order to be used at its full lightweight potential, Usibor®1500 crash ductility must be characterized and modeled properly.
The usual Usibor®1500 failure modelling method proposed by ArcelorMittal always remains compatible with a current full car model mesh size, whether for base metal, spotweld Heat Affected Zone (HAZ) or laser welded line. A CrachFEM fracture criterion applied on 3 mm – 5 mm shell elements mesh size (even if geometry size is lower than the used mesh size) is one possibility.
A meso-scale finite element model is sometimes required either to improve failure prediction accuracy, or to obtain equivalent failure parameters for a following full car model simulation. Three solutions are then possible if a heterogeneous model including standard size shell elements for the vehicle and finer 3D solid elements is realized:

- Use an imposed time step close to the shell elements one's, with the risk to obtain results affected by an excessive added mass on the finest 3D elements used locally for the failure prediction.
- Build a sub-model including the finest 3D-elements and apply imposed velocities at the border. These velocities are extracted from the full car model. This method can be assimilated to the super-element method during a linear analysis. If it provides some good results in case of a front-end module during a front crash, applying it on a B-pillar during a side impact is much more complicated.
- Use the subcycling or multiscale options that allow running the crash simulation with several time steps adapted to the different areas mesh size.

The last solution is retained to simulate parts failure prediction during crash on a full vehicle model. New features like Subcycling - **`*CONTROL_SUBCYCLE_K_L`** - and Multiscale - **`*CONTROL_SUBCYCLE_MASS_SCALED_PART_{SET}`** recently developed by LSTC and DYNAmore (2014) can accommodate this need. The results obtained with LS-DYNA® version V980_R9.0.1 [1] which includes the latest possibilities of these two features is proposed in this paper.

2 Interest of multi time stepping methods

In an explicit time integration computation, the stable time step is determined by the smallest element length (L) as given by *equation 1*:

$$\Delta t = \frac{L}{c} = L \times \sqrt{\frac{\rho}{E}} \quad \textit{Equation (1)}$$

The major drawback for a heterogeneous model, is that a few number of small elements can penalize the computation time. The user can, of course, impose a higher time step to whole model in order to reduce the computation time. In this case, the risk to change locally the physics (plastic strain especially) if the mass scaling becomes ambitious (too high ρ value in equation1).

Some methods called multi time stepping or Subcycling were developed forty years ago, [2, 3] to distribute nodes or elements into sub models with contact treatment between domains. Each one will use its own time step.

One of these algorithms combining stability and results accuracy has been already available in LS-DYNA for many years. It was recently updated [4], as the growing need in the automotive industry for an accurate failure prediction during crash simulation.

2.1 Multi time stepping methods applied on a S-rail model

The multi time stepping methods will be tested first on an S-rail model, very similar to one used in the subcycling performances assessment study presented in 2014 [4].
The S-rail model is composed of a hat section and a closing plate welded with 35 spotwelds. The goal is to estimate the computation time saving, stability and results accuracy on a simple geometry that presents similar nodes distribution ratios compare to a full car model, into the different sub domains.
This heterogeneous S-rail model presented figure 1 is composed of:

- A hat section: 7700 shell elements (21.7%) - 7920 nodes, 5 mm mesh size commonly used for a full car crash simulation.
- A closing plate: 25724 shell elements (72.4%)-26220 nodes, 2 mm mesh size (3mm is currently used for a CrachFem failure assessment).
- One refined spotweld close to the plastic hinge area: 2048 solids (5.7%), 2601 nodes, 0.25 mm mesh size which is slightly less to the expected target for a refined local area [0.3mm; 0.5 mm].
- 34 spotwelds: 1-HEX solids (0.001%), 272 nodes.

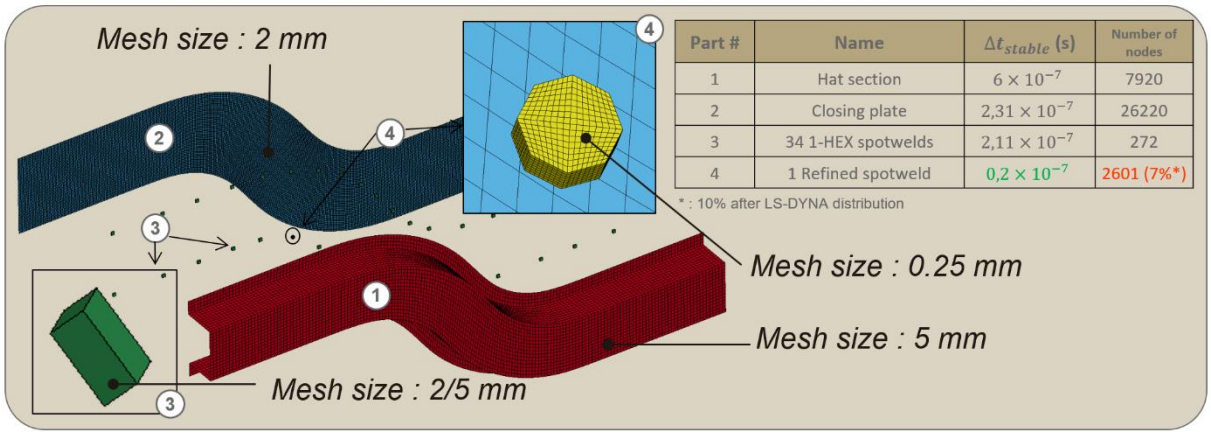

Part #	Name	Δt_{stable} (s)	Number of nodes
1	Hat section	6×10^{-7}	7920
2	Closing plate	$2{,}31 \times 10^{-7}$	26220
3	34 1-HEX spotwelds	$2{,}11 \times 10^{-7}$	272
4	1 Refined spotweld	$0{,}2 \times 10^{-7}$	2601 (7%*)

* : 10% after LS-DYNA distribution

Fig.1: S-rail model, number of nodes and corresponding time steps.

Results quality and computation time saving will be assessed for both Subcycling and Multiscale methods. The plastic strain level will be especially observed around the refined spotweld to estimate some possible mass scaling negative effects.

2.1.1 Subcycling method

The Subcycling method is called by ***CONTROL_SUBCYCLE_K_L** card. It contains two parameters, K and L:

- K can take the following values: 1, 2, 4, 8, 16, 32 or 64 and represents the maximum scale factor between the time step of one node and the smallest time step in the model. It is also linked to the number of sub domains *m* by the relationship: $K = 2^{m-1}$. The nodes are then distributed into m groups, each one will run with its own time step. Default value is K=16.
- L gives the maximum number of time steps for external force calculations, including penalty contacts. The parameter L should be less than or equal to K. The default value is L=1.

The parameter L was set to 1 in a first step (external forces computed at each time step) while parameter K variations are in the range [2; 64]. Nodes distribution presented in table 1, already shows that SUBCYCLE_32_1 and SUBCYCLE_64_1 will provide same results.
Minimum retained time step is the smallest one: $2.0*10^{-8}$ s.
The nodes distribution in the different time step groups (table 1) is globally consistent with the number of nodes in each part presented figure 1.
Nevertheless, a small difference on the lowest time step group is observed: it contains more nodes (3728) than the expected number (2601).

Configuration	1* ΔT	2* ΔT	4* ΔT	8* ΔT	16* ΔT	32* ΔT	64* ΔT
SUBCYCLE_2_1	3728	33285	0	0	0	0	0
SUBCYCLE_4_1	3728	0	33285	0	0	0	0
SUBCYCLE_8_1	3728	0	0	33285	0	0	0
SUBCYCLE_16_1	3728	0	0	8526	24759	0	0
SUBCYCLE_32_1	3728	0	0	8526	17403	7356	0
SUBCYCLE_64_1	3728	0	0	8526	17403	7356	0

Table 1: Nodes distribution on the different groups for K values between [2;64]

Results quality are first estimated for different K and L variations:

- Similar S-rail internal energy level is obtained for all K values between [2; 64] (600 J, figure 2)
- Identical internal energy level is obtained for L in the range [2; 32], while K is fixed to 32 (right curves, figure 2).
- Plastic strain contours close to the refined spotweld are exactly the same for all K values and identical to the contours obtained with only one smallest time step (figure 3). A computation was also performed with one imposed time step equal to $7*10^{-7}$ s. (value usually used for mesh size 5mm) to estimate the negative effect of an ambitious time step: plastic strain level close to refined spotweld becomes higher due to huge amount of added mass compared to subcycling computations (figure 3).

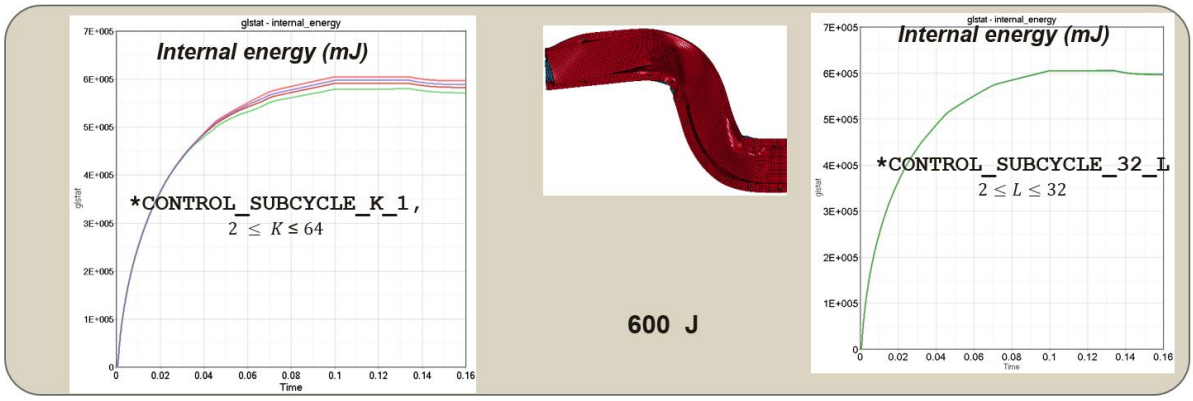

Fig.2: Internal energy vs. time for a K variation (left), L variation (right)

The curve representative of the computation time saving vs. K value is presented figure 4.
The maximum time saving reaches 62% without any mass scaling, with L=1.
Computation time saving is less sensitive to L variations: -62% for ***CONTROL_SUBCYCLE_32_2** vs. -64% for ***CONTROL_SUBCYCLE_32_32.**

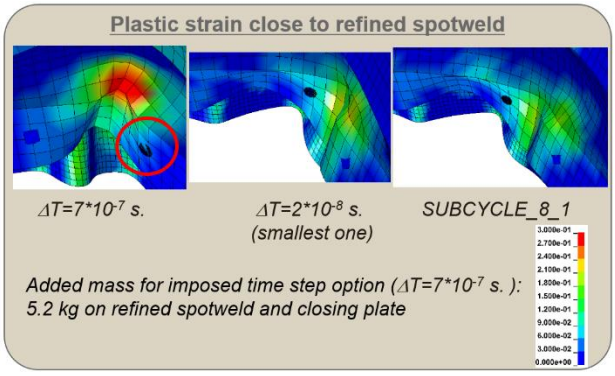

Fig.3: Plastic strain contours in the plastic hinge area

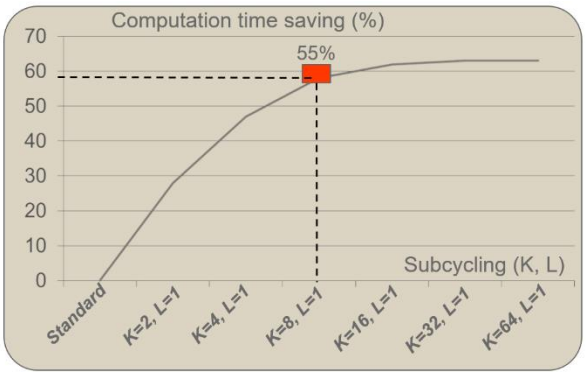

Fig.4: Computation time saving for K values between [2,64]

Standard ($2*10^{-8}$ s.)	***CONTROL_SUBCYCLE_K_L**	Imposed time step (5mm, $7*10^{-7}$ s.)
864 min.	311 min.< _K_L < 600 min.	27 min.

Table 2: Elapsed time comparison between subcycling and standard computation (MPP, 16 CPUs).

To conclude this section, if the Subcycling method provides a significant time saving (311 min for the faster computation vs. 864 min without), the negative impact of the refined mesh size area on computation time is important: it has to be recalled that the elapsed time was 27 minutes for an imposed time step equal to $7*10^{-7}$ s. (table 2).

*2.1.2 Multiscale option: ***CONTROL_SUBCYCLE_MASS_SCALED_PART_{SET}***

In this context, the user determines the time step and the corresponding mass scaling of one part or a set of parts if option **_{SET}** is added.
Several combinations were tested with or without mass scaling.
A very good compromise between computation time and results quality were obtained with following imposed time steps (table 3). Note that these time steps are close to the stable ones except the smallest time step for the refined area: $3.75*10^{-8}$ s. was imposed vs $2.0*10^{-8}$ s. for the stable one.

***CONTROL_SUBCYCLE_MASS_SCALED_PART**			
Hat section	Closing plate	34 spotwelds	1 refined spotweld
$6.0*10^{-7}$ s.	$3.0*10^{-7}$ s.	$3.0*10^{-7}$ s.	$3.75*10^{-8}$ s.

Table 3: Imposed time step for the different S-rail parts - 2^m ratio between time steps

The corresponding nodes distribution into groups *1/ *2/ *4/ *8/ *16/ *32/ *64 becomes the following:
3728 / 0 / 0 / 25668 / 7617 / 0 / 0
Same remark can be made about nodes distribution: 3728 nodes are put on the smallest time step group instead of 2601 expected. This will have a small negative impact on computation time.

The computation time for this configuration with a ratio between smallest and higher time step equal to 16, is 201 min: the time saving reaches 77% compared to standard simulation with $2*10^{-8}$ s. time step.
With a ratio equal to 8 without any mass scaling -smallest time step is then set to $2.0*10^{-8}$ s.- the elapsed time becomes 354 min. (-60%).

Similar energy absorbed curve and no additional plastic strain close to the refined spotweld due to added mass is observed (+0.025 kg, figure 5).

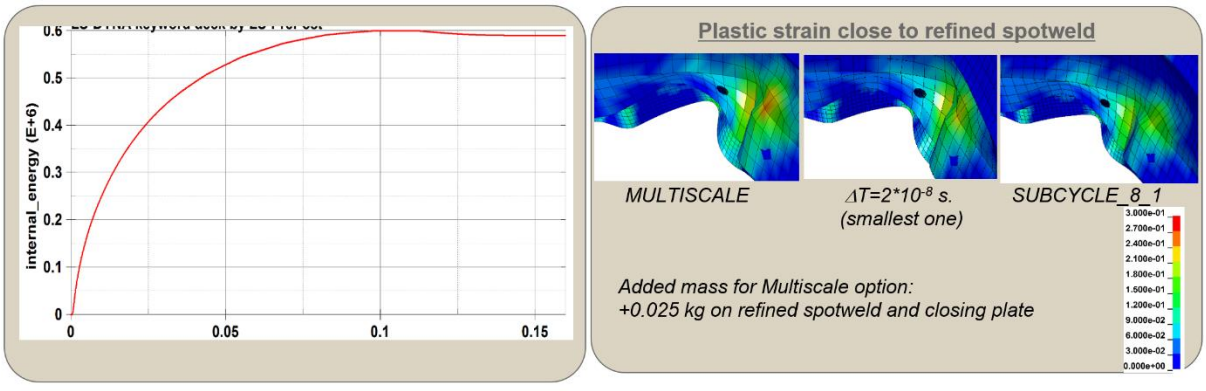

Fig.5: Energy absorbed (multiscale configuration) and Plastic strain contour in the plastic hinge area

To conclude this section, the multiscale approach is more appropriate to a local failure analysis as the user has the control of the nodes distribution into sub domains.
It will be used with a maximum time step ratio equal to 8 corresponding to the ratio between a refined 3D mesh size [0.3mm; 0.5 mm] and a global domain composed of 3 mm shells. The estimated

computation time saving potential reaches 60% if the number of small elements represent 7% of total elements. For a ratio equal to 16, the potential would reach 77%.

3 2D-3D transition area modeling

The multi-scale approach applied on a heterogeneous crash model, will require a transition area between the finest 3D mesh (0.25-0.5 mm mesh size for the presented industrial examples) and the coarse shell mesh usually used in a full car model (3mm-5 mm).
A solution composed of shell elements penetrating through the solids with an additional tied interface is possible. The retained solution B, presented figure 6, is made of 2D transition area with one node used as master node of the ***CONSTRAINED_INTERPOLATION** card containing slave nodes that belong to solids. It is automatically generated with a Python tool. To simplify reading of the current article, ***CONSTRAINED_INTERPOLATION** card will be called RBE3, as denominated in NASTRAN.
The bending and torsional elementary performances of this mixed beam is compared to the full 3D solution. The results (displacements, stresses) are quite good with a difference lower than 2%. Moments transmission from 6-degrees of freedom (dof) shell elements to 3 dof solids is guaranteed.
The alternative C (figure 6) with an added orthogonal plate without any RBE3 for moments transmission is also presented. The bending performance is similar to the full solids modeling one (gap lower than 2%), while the torsional stiffness is a little bit far (14%).

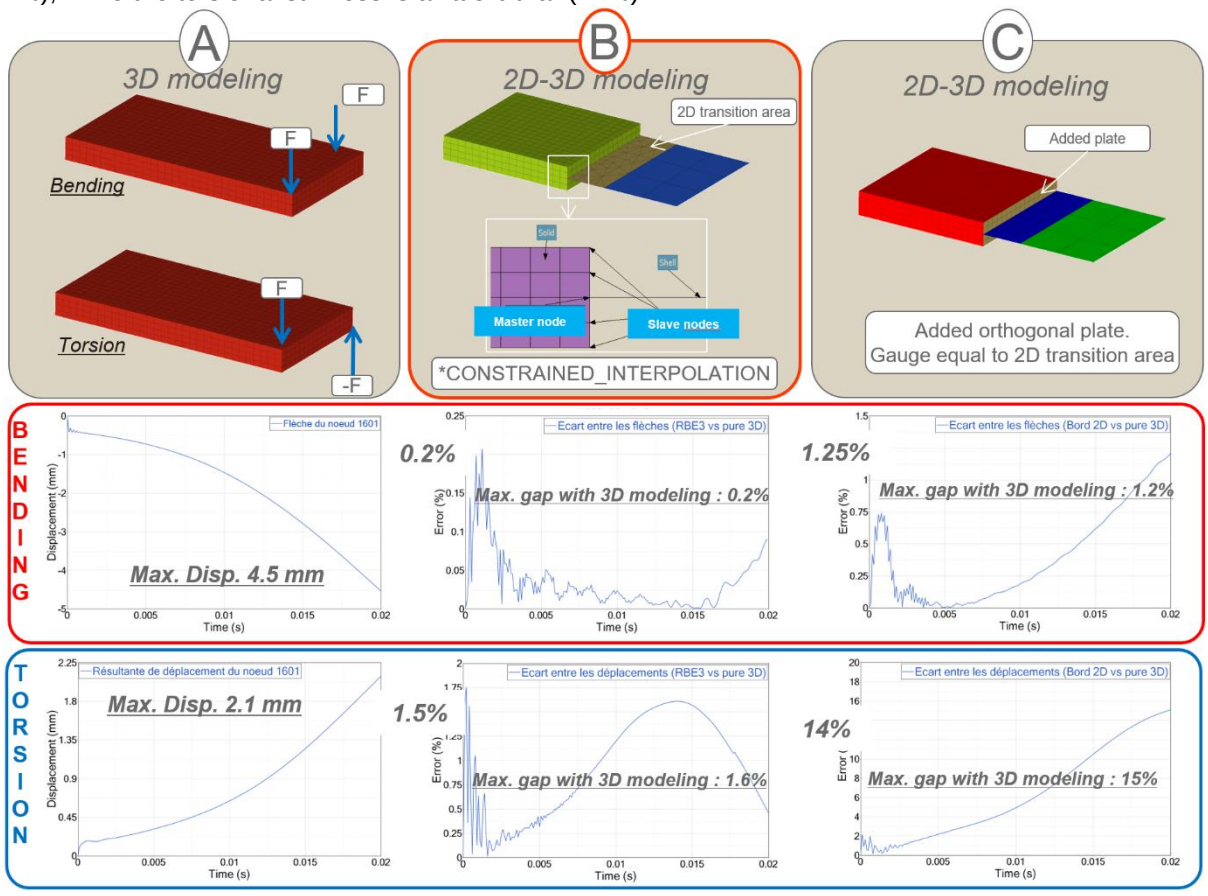

Fig.6: 2D-3D transition area modeling and obtained gap vs 3D modeling displacement

Then, option B with ***CONSTRAINED_INTERPOLATION** card is the best solution to transmit moments from shell elements to 3D-elements. Unfortunately, some issues with option B used with LS-DYNA® version V980_R9.0.1 were observed when one node that belongs to this RBE3 becomes a free-node. This happens when a solid that contains this node is deleted due to failure. It is the reason why option C will also be retained temporarily to obtain a normal termination on a full crash simulation.

4 Multiscale application on a spotweld Heat Affected Zone (HAZ) failure prediction during 3 points bending test.

This application was performed on a 3-points bending sample for which some physical tests results are available in ArcelorMittal. This will allow to compare performances relatively to physical test, current simulation and meso-scale model with multiscale approach before applying the methodology on full car model.

4.1 Issue and context

Press Hardening Steels (PHS) reach their final mechanical properties thanks to thermal treatment during the hot forming process (quenching after austenitization). During the assembly of hot formed parts, spotwelding causes a new local heat treatment with a relatively slow cooling in the Heat Affected Zone (HAZ) that induces softening of the material around the weld (figure 7).
This is a weak point in the steel sheet because of its lower hardness: strain could localize in the HAZ leading to early cracks.

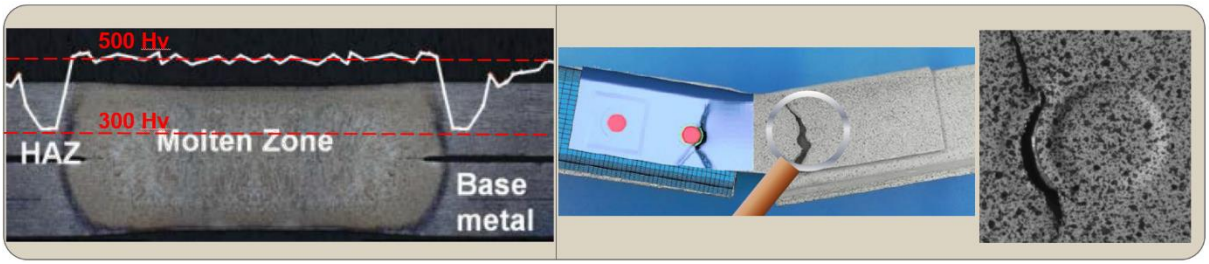

Fig.7: Hardness profile on Usibor®1500 spotweld and early failure scenario caused by HAZ softening

4.2 Spotwelds HAZ modeling

The component proposed for this spotweld HAZ failure assessment is used within FOSTA project [5]. It is made of two hat shape profiles welded with two L profiles (see figures 7 and 9). It is then loaded under three-points-bending.

4.2.1 Current modeling

The ArcelorMittal classical modeling rules for failure prediction are the following:
- Shell elements, 3mm mesh size for both base metal and HAZ.
- USIBOR®1500 CrachFem [6] material card is applied on base metal and molten zone. Three failure modes are accounted:
  - Ductile Normal Fracture (DNF)
  - Shear ductile fracture.
  - Instability (necking). This failure mode will lead to HAZ failure.
- Use of 72% of the USIBOR®1500 material card scaling on hardening profile for the HAZ. This is an important parameter as the strain localization in the softened HAZ dominates the fracture strain rather than strain path.

4.2.2 Meso-scale model presentation

Description of the 2D-3D meso-scale model:
- Two spotwelds of the sample are modeled with 3D elements. The mesh size is in the range [0.25 mm; 0.50 mm]. Each spotweld also, called macro-element, is composed of 22700 elements including the 2D-transition area elements (*figure 8*).
- The 2D-3D transition area is using RBE3 modeling to transmit the moments (option B presented in section 3). 300 RBE3 per spotweld are necessary to connect 2D shell elements to 3D-solid elements. They are created thanks to a Python script.
- The material card used for the base metal is **`*MAT_PIECEWISE_LINEAR_PLASTICITY`** with **`*MAT_ADD_EROSION`** [7,8].
- Same material card is used for HAZ, with a scale factor equal to 72% applied on (σ,ε) curves of base metal. As three solids elements are used in the ring width, a finer hardness profile discretisation would be possible but not tested in the presented simulation.
- HAZ ring width is set to 1.5 mm, and modeled with 3 solids elements.

- Both nuggets (diameter 5 mm) are connected with ***CONSTRAINED_NODAL_RIGID_BODY** (see figure 8).
- Time step ratio between smallest 3D elements and shell elements is set to 8: ***CONTROL_SUBCYCLE_MASS_SCALED_PART_SET** card is used on 3D elements and transition area with an imposed time step equal to 3.0E-8 s. For all other parts, the imposed time step DT2MS of ***CONTROL_TIMESTEP** card is set to 2.4E-07s.

Time steps and nodes distribution are presented in *table 4.*

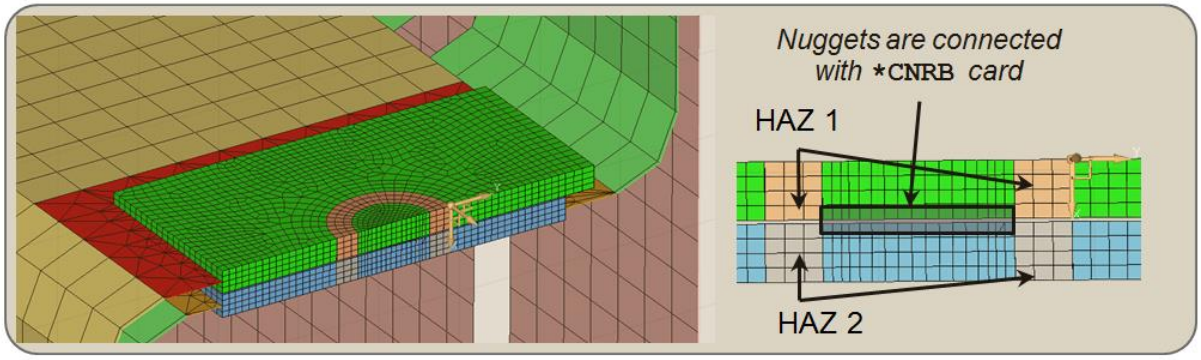

Fig.8: One spotweld macro-element composed of 22700 solids and shells for transition area

Mesh size	Number of nodes	Stable time step Imposed time step	Percentage vs total nodes	Nodal partitioning for subcycling
3D elements [0.25 mm – 0.50 mm]	45514	2.7E-08 s. 3.0E-08 s.	74.5%	52394 (85.9%)
Shell elements [3.0 mm – 3.0 mm]	15623	2.4 E-07 s (*8)	25.5%	8601 (14.1%)

Table 4: Nodes distribution and corresponding time steps.

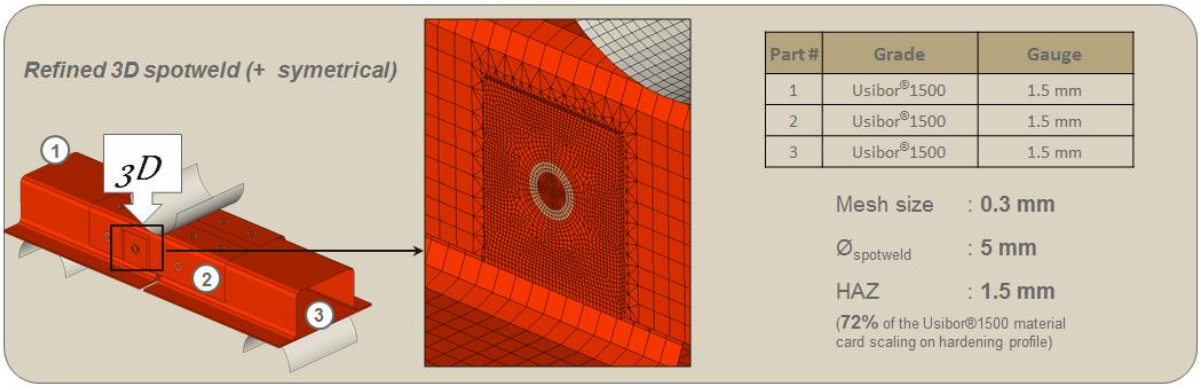

Fig.9: Three points bending test meso-scale model realized for spotweld HAZ failure prediction

4.3 Meso-scale model results

4.3.1 Results quality

The spotweld HAZ failure was well predicted for a cylinder displacement equal to 13 mm. Similar value was obtained during physical test. The meso-scale model has also confirmed the CrachFem result obtained with the shell elements model.
A comparison between the multiscale computation and a classical simulation with only one time step equal to the smallest one (DT2MS equal to 3.0E-07 s in ***CONTROL_TIMESTEP** card) leads to the same result (see *figure 10*).
A very good agreement is observed with physical test results presented figure 8 in paper [5].

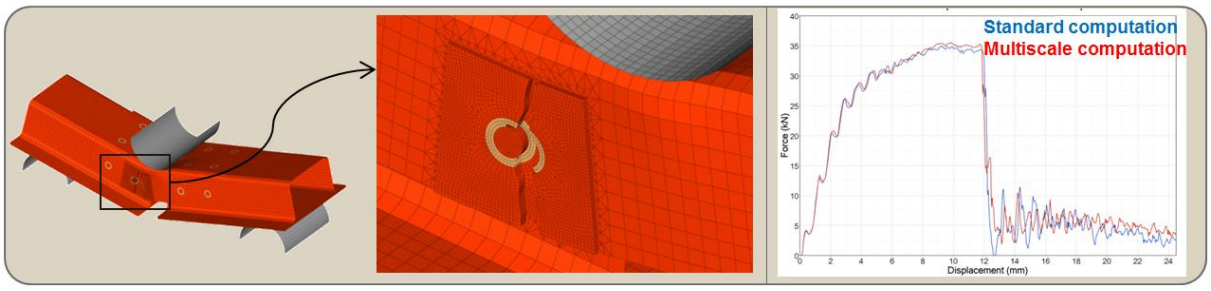

Fig.10: Deformed shape and force vs displacement curve

4.3.2 Computation time saving efficiency and comments.

The efficiency of the multiscale computation is of course not optimal for this learning case: time saving is less than 2% in the multiscale computation compared to standard computation with only one time step DT2MS set to 3.0E-08 s. *(table 5*).
The reason is the too high percentage (75%) of 3D elements that run with the smallest time step vs the total number of elements (see *table 4*).
Moreover, it is also observed in table 4 that the nodal partitioning done by LS-DYNA is unfavourable: nearly 86% of the total number of nodes is running with the smallest time instead of 75% expected.

Computation	Imposed time step	Elapsed time	Time saving
Multi-scale	3.0E-08 s. 2.4E-07 s.	2h07min	1.5%
Standard	3.0E-08 s.	2h09 min	

Table 5: Elapsed time comparison between multiscale and standard computation (MPP, 64 CPUs).

5 Multiscale application on spot-welds Heat Affected Zone (HAZ) failure prediction on S-in motion® Mid-size Sedan during IIHS side impact.

In this section, the S-in motion® Mid-size Sedan full car model, developed internally to promote the new ArcelorMittal steel grades to its customers [9], is used to assess failure risks on spotwelds HAZ.
A first IIHS side impact simulation with 4-HEX spotwelds with HAZ shell ring was performed with modeling rules presented in paragraph *4.2.1 current modeling* of the previous section.
Six HAZ spotwelds on the B-pillar inner lower area were considered as critical. They are located in front of the DUCTIBOR® 500 area (see *figure 11*) where the plastic hinge occurs.
A macro-element composed of approximately 8000 solids and shells for transition area is representing one spotweld (see *figure 12*). Duplicated six times, they are replacing the spotwelds that were estimated as critical in the first simulation.

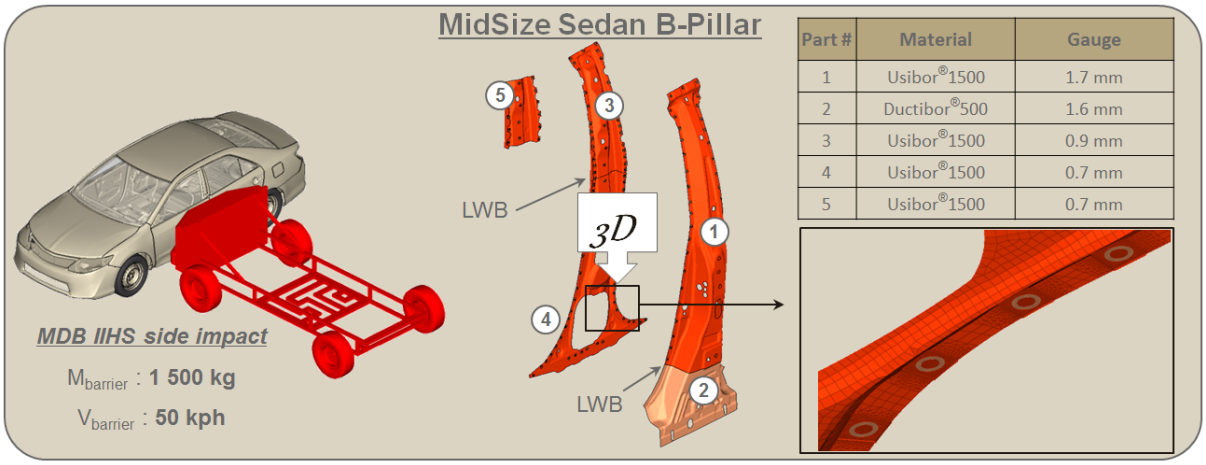

Fig.11: 2D-3D spotwelds HAZ failure assessment on S-in Motion® Mid-size Sedan B-pillar

5.1 Spotwelds HAZ meso-scale model presentation

The spotweld HAZ mesh size is in the range [0.25 mm-0.5 mm]. The meso-scale description is identical to that presented in section *4.2.2.* except on the two following points:

- ***CONTROL_SUBCYCLE_MASS_SCALED_PART_SET** card is used on 3D elements and transition area with an imposed time step equal to 5.0E-8 s. For all other parts, the imposed time step DT2MS of ***CONTROL_TIMESTEP** card is set to 4.0E-07s. Ratio of 8 between both time steps is maintained.
- An orthogonal part made of shells (alternative C presented in section 3) is used to transmit moments from shells 3mm mesh size to solid elements (see figure 12). Previous computation using ***CONSTRAINED_INTERPOLATION** card failed before end of crash: some nodes belonging to RBE3 become free node as soon as one element is deleted due to failure that occur in the 3D elements.

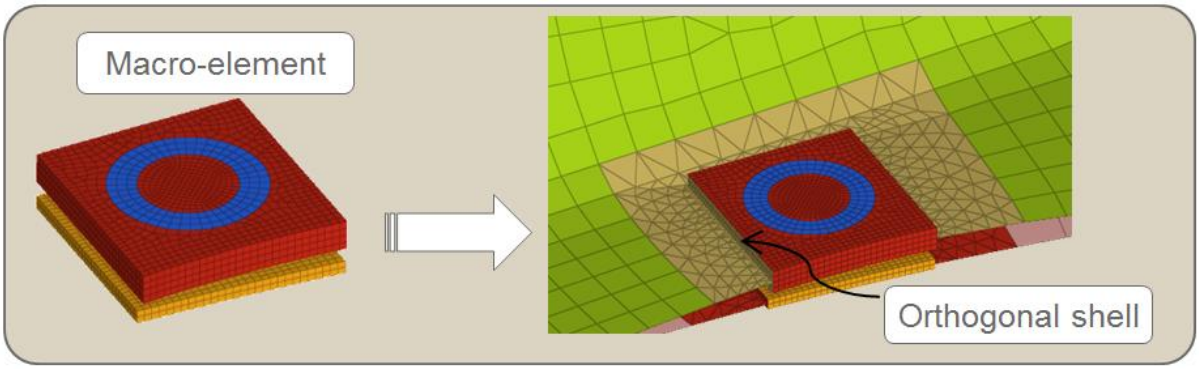

Fig.12: The 3D spotweld macro-element with transition shells

Time steps and nodes distribution are presented in table 6.

Mesh size	Number of nodes	Stable time step Imposed time step	Percentage vs total nodes	Nodal partitioning for subcycling
3D elements [0.25 mm – 0.50 mm]	47566	2.5E-08 s. 5.0E-08 s.	2.3%	292361 (14%)
Full vehicle model [3.0 mm – 5.0 mm]	2 018 086	1.0 E-07 s 4.0 E-07 s (*8)	97.7%	1775190 (86%)

Table 6: Nodes distribution and corresponding time steps.

5.2 Meso-scale model results

5.2.1 Results quality

3D multiscale and one-time-step simulations have provided the same results: failure is initiated in 3D-spotwelds HAZ after 15 ms. Both simulations confirmed results initially obtained with 4-HEX spotwelds and shell HAZ modeling with CrachFem material laws.

Thanks to these 3D meso-scale models, design changes were brought to B-pillar inner lower area especially nearby the seatbelt retractor hole. This has led to a safe B-pillar as confirmed by the physical test performed on a B-pillar unit, till an intrusion level similar to that observed in the full car model (figure 13).

Fig.13: Improved B-pillar with safe lower area thanks to design modifications.

5.2.2 Computation time saving efficiency and comments.

The computation time saving reaches 28% with multiscale option compared to standard one (see table 7). This is less than the expected value due to nodal partitioning: 14% of nodes ran with the smallest time step (5.0E-08 s) instead of 2% expected (*table 7*). Same observation was done on the 3-points sample and the S-rail nodal partitioning.

Computation	Imposed time step	Elapsed time	Time saving
Multi-scale	5.0E-08 s. 4.0E-07 s.	44h35min	28%
Standard	5.0E-08 s.	62h51 min	-

Table 7: Elapsed time comparison between multiscale and standard computation (MPP, 64 CPUs).

6 Multiscale application on a laser welded line failure prediction on S-in motion® C-segment B-pillar during AEMDB side impact.

6.1 Context

Laser welded blanks consists to weld two materials with different steels grades and thicknesses (t_1, t_2) through the use of laser technology. The technical delivery conditions are defined by the standard EN 10359 “Laser welded tailored blanks — Technical delivery conditions”.
The main criteria used for the weld geometry are (figure 14):

1. $t2 \leq 1$ mm: $h \leq 0{,}1$ mm,
2. $t2 > 1$ mm: $h \leq 0{,}1 \times t2$
3. $t2 \leq 1$mm: $g \geq 0{,}80 \times t2$
4. $t2 > 1$ mm: $g \geq 0{,}80 \times t2$

Where t_2 is thinner material, h weld geometry defect and g remaining weld thickness

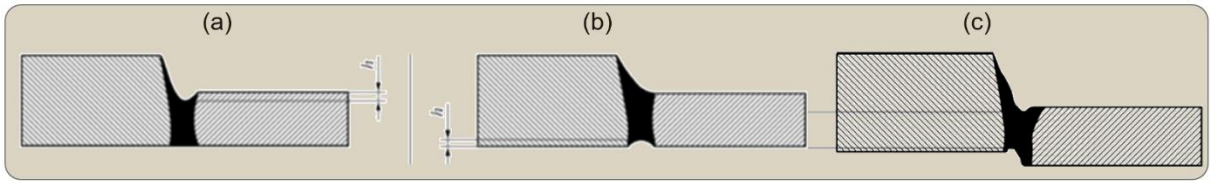

Fig.14: Weld geometry defect (a) Upper weld concavity (b) Lower weld concavity (c) Weld cross section

To avoid high weld geometry defect, ArcelorMittal propose enable technologies including compensation of missing material due to cut edge quality by filler wire. Filler wire is recommended when thickness difference is below 0.2 mm to better compensate gap and missing material [10].
A meso-scale FE model is realized on a weld geometry of Laser Welded Blank (LWB) line:

- 85% of the smallest gauge between both blanks which is severe compared to typical production quality. The remaining cross section due to weld defects (Undercut, Root concavity, Upper weld concavity).
- The LWB line width is set to 1 mm.

This LWB line meso-scale model is applied on the S-in motion® C segment B-pillar during an AEMDB side impact (figure 14 and [11]). A more critical LWB PHS B-pillar proposal was built to assess failure risk for the line: B-pillar lower area steel grade is moved from Ductibor500 to USIBOR®1500.

6.2 LWB line meso-scale model presentation.

Description of the 2D-3D Laser Welded Blanks (LWB) line meso-scale FE model:

- The material card used for the USIBOR®1500 base metal is **`*MAT_PIECEWISE_LINEAR_PLASTICITY`** with **`*MAT_ADD_EROSION`** [7,8].
- An orthogonal part made of shells (alternative C presented in section 3) is used to transmit moments from shells 3mm mesh size to solid elements (figure 15), for the reason explained in section 5.1.

- ***CONTROL_SUBCYCLE_MASS_SCALED_PART_SET** card is used on 3D elements and transition area with an imposed time step equal to 5.0E-8 s. For all other parts, the imposed time step DT2MS of ***CONTROL_TIMESTEP** card is set to 4.0E-07s. Ratio of 8 between both time steps is maintained.

Time steps and nodes distribution are presented in *table 8.* As observed in previous examples, number of nodes running with the smallest time step (469083) is significantly higher than the number of nodes contained in the 2D-3D refined area (133612).

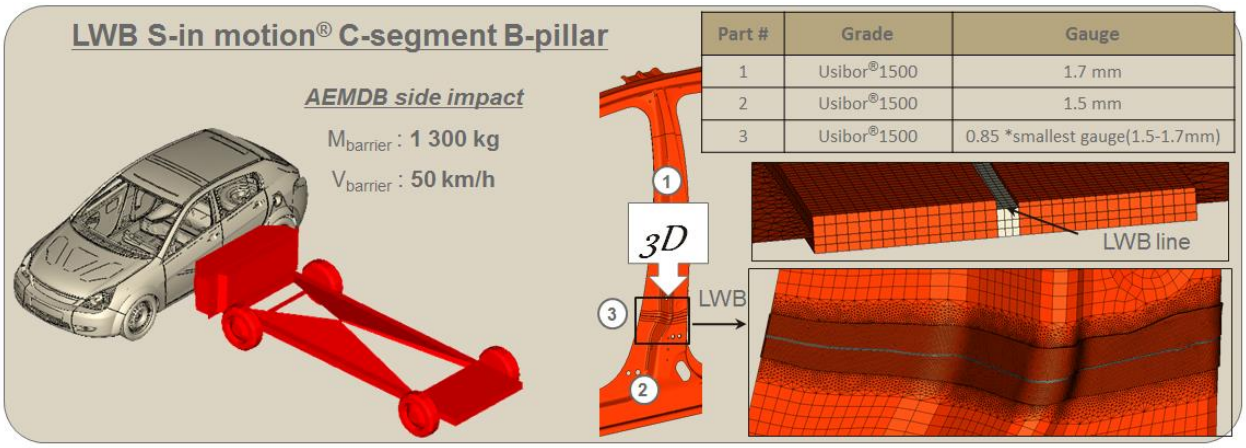

Fig.15: 2D-3D LWB line failure assessment on the S-in Motion® C-segment B-pillar

Mesh size	Number of nodes	Stable time step Imposed time step	Percentage vs total nodes	Nodal partitioning for subcycling
3D elements [0.33 mm – 0.5mm]	133612	2.8E-08 s. 5.0E-08 s.	4.8%	469083 (14%)
Full vehicle model [3 mm – 5mm]	2 646 233	1.0 E-07 s 4.0 E-07 s (*8)	95.2%	2311851 (86%)

Table 8: Nodes distribution and corresponding time steps.

6.3 Meso-scale model results

6.3.1 Results quality

Two computations with multiscale option and standard simulation with only one time step have provided the same result: plastic strain distribution in the LWB line refined area was observed, energy absorbed as well (figure 16). The LWB line is safe after AEMDB side impact crash.
This result was also compared with the initial shell model without any USIBOR®1500 failure model: The observed plastic hinge for shell model and meso-scale models is exactly the same (figure 16).

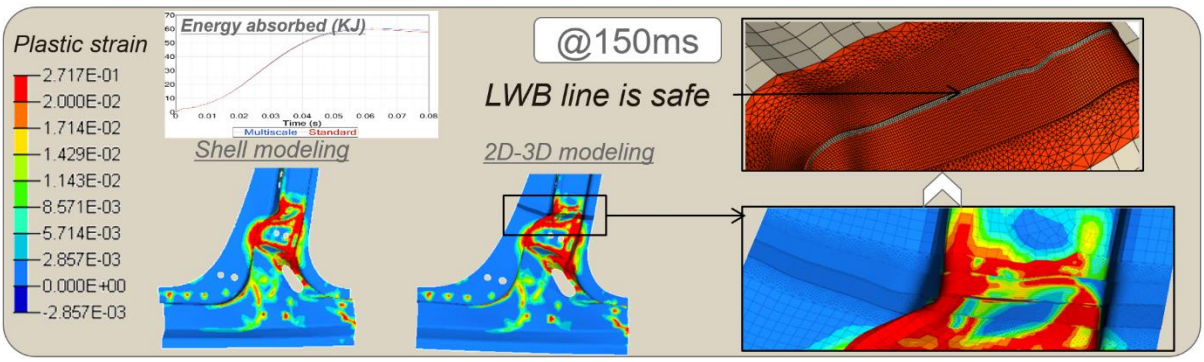

Fig.16: Meso-scale deformed shape vs shell modeling. The LWB line is safe @end of side impact

6.3.2 Computation time saving efficiency and comments.

The computation time saving reaches 34% with multiscale option compared to standard one (table 9). This is significantly less than the expected value for the reason given in section *5.2.2*: 14% of nodes ran with the smallest time step (5.0E-08 s) after nodal partitioning instead of 5% expected (*table 9*).

Computation	Imposed time step	Elapsed time	Time saving
Multi-scale	5.0E-08 s. 4.0E-07 s.	36h25min	34%
Standard	5.0E-08 s.	54h47 min	-

Table 9: Elapsed time comparison between multiscale and standard computation (MPP 64 CPUs).

7 Summary

A multi-scale methodology using ***CONTROL_SUBCYCLE_MASS_SCALED_PART_SET** card could be an interesting alternative when an equivalent failure behavior used with a coarse shell modeling is not sufficient: it can substantially reduce elapsed time in case of a heterogeneous model composed of a very fine mesh size area for a local failure assessment during a full car crash simulation:

- The efficiency of the methodology is increased by the fact that ratio γ between nodes running with the smallest time step and the total number of nodes is low: time saving can reach 34% in case of a favorable γ ratio equal to 5%.
- Result quality is identical to those obtained with a classical method based on one imposed smallest time step DT2MS selected in ***CONTROL_TIMESTEP** card.
- Plastic strain level in the finest mesh size area is not impacted by mass scaling as it could be if the highest time step was imposed to whole elements.

Guidelines and limitations:

- Maximum time step ratio between smallest 3D elements, with mesh size between [0.3mm;0.5mm] and shell elements [3mm;5mm] was set to 8 to avoid any instability risks and seemed more appropriate to this mesh size ratio than factor 16 considered as too ambitious.
- The nodal partitioning for subcycling done by LS-DYNA: 14% of total number of nodes ran with the smallest imposed time step while 5% of them only was expected: the time saving could be higher than the presented value (34%).This is significantly less than the expected value (55%) obtained in the S-rail model with similar ratio γ.
- Nevertheless, it must be kept in mind that the meso-scale model computation time is much higher than the one observed for the coarse mesh without any refined area: computation time obtained for D-segment full vehicle with multiscale option was equal to 44H35 vs 28H31 without any refined area (62H51 for the refined area computation running with the smallest time step).

One issue encountered on 2D-3D transition area modeling with LS-DYNA® version V980_R9.0.1:

- Abnormal termination occurs if a node belonging to one RBE3 (***CONSTRAINED_INTERPOLATION** card) becomes a free node as it is observed after a 3D element deletion due to failure. An alternative solution with an orthogonal plate was temporarily used.

8 Literature

[1] Livermore Software Technology Corporation, LS-DYNA® Keyword User's Manual, vol. 1, Livermore, 2016.

[2] T. BELYTSCHKO, H. J. YEN et R. MULLEN, Mixed methodes for time integration, 1979.

[3] G. M. Hulbert et T. J. Hughes, Numerical evaluation and comparison of subcycling algorithms for strutural dynamics, 1988.

[4] T. BORRVALL, D. BHALSOD, J.O. HALLQUIST, B. WAINSCOTT, “Current Status of Subcycling and Multiscale Simulations in LS-DYNA®” . 13th International LS-DYNA users Conference 2014, Dearborn, Michigan, USA, 2014

[5] S. BURGET, S. SOMMER Fraunhofer IWM Freiburg, “Characterization and modelling of fracture behavior of spotwelded joints in hot-stamped ultra-high strength steels”. LS-DYNA Forum, Ulm, 2012

[6] MF GenYld + CrachFem3.8 user's Manual, MATFEM,2008
[7] G. HUANG, H.ZHU, S.SADAGOPAN, Y. CHEN, C. XIA, O. FARUQUE, "Fracture Prediction and Correlation of AlSi Hot Stamped Steels with Different Models in LS-DYNA®", 13th International LS-DYNA users Conference 2014, Dearborn, Michigan, USA, 2014
[8] Y. CHEN,O. FARUQUE, C. XIA, A. AKKERMAN, D. LAM, "Meso-Scale FEA Modeling to Simulate Crack Initiation and Propagation in Boron Steel", 13th International LS-DYNA users Conference 2014, Dearborn, Michigan, USA, 2014
[9] I. VIAUX, F. ARNAUTU, "Lightweight steel Mid-size Sedan and SUV bodies", Aachen Body Engineering Days 2016, Aachen, 2016
[10] F. SCHMIT, S. GAIED, M.I. ROTARESCU, G. TANDON, "Butt laser welding of AlSi coated Press Hardened Steels – New developments and applications", IABC Conference 2016, Dearborn, Michigan, USA, 2016
[11] P. DIETSCH, D. HASENPOUTH, "Crash ductility and numerical modeling of Usibor1500® fracture behaviour", IABC Conference 2016, Franckfurt, 2015